

# UC Irvine

## UC Irvine Previously Published Works

### Title

New insights into secondary organic aerosol from the ozonolysis of  $\alpha$ -pinene from combined infrared spectroscopy and mass spectrometry measurements.

### Permalink

<https://escholarship.org/uc/item/1tb933gr>

### Journal

Physical chemistry chemical physics : PCCP, 16(41)

### ISSN

1463-9084

### Authors

Kidd, Carla  
Perraud, Véronique  
Finlayson-Pitts, Barbara J

### Publication Date

2014-11-07

Peer reviewed



Cite this: *Phys. Chem. Chem. Phys.*,  
2014, **16**, 22706

# New insights into secondary organic aerosol from the ozonolysis of $\alpha$ -pinene from combined infrared spectroscopy and mass spectrometry measurements

Carla Kidd, Véronique Perraud and Barbara J. Finlayson-Pitts\*

Understanding mechanisms of formation, growth and physical properties of secondary organic aerosol (SOA) is central to predicting impacts on visibility, health and climate. It has been known for many decades that the oxidation of monoterpenes by ozone in the gas phase readily forms particles. However, the species responsible for the initial nucleation and the subsequent growth are not well established. Recent studies point to high molecular weight highly oxygenated products with extremely low vapor pressures (ELVOC, extremely low volatility organic compounds) as being responsible for the initial nucleation, with more volatile species contributing to particle growth. We report here the results of studies of SOA formed in the ozonolysis of  $\alpha$ -pinene in air at  $297 \pm 2$  K using atmospheric solids analysis probe (ASAP) mass spectrometry, attenuated total reflectance (ATR) Fourier transform infrared spectrometry and proton transfer reaction (PTR) mass spectrometry. Smaller particles are shown to be less volatile and have on average higher molecular mass components compared to larger particles, consistent with recent proposals regarding species responsible for the formation and growth of particles in this system. Thus the signatures of species responsible for particle development at various stages are observable even in particles of several hundred nm diameter. Pinonaldehyde and acetic acid were observed to evaporate from a film of impacted SOA at room temperature, from which the ratio of their diffusion coefficients to the square of the average film thickness,  $D/l^2$ , could be obtained. For acetic acid and pinonaldehyde,  $D/l^2 = 6.8 \times 10^{-6} \text{ s}^{-1}$  and  $5.0 \times 10^{-6} \text{ s}^{-1}$  respectively, the relative magnitudes being consistent with the size difference between acetic acid and pinonaldehyde molecules. Limitations to quantifying the film thickness and hence absolute values of the diffusion coefficient are discussed and highlight a need for novel experimental methods for quantifying diffusion coefficients of organic species in SOA.

Received 31st July 2014,  
Accepted 12th September 2014

DOI: 10.1039/c4cp03405h

[www.rsc.org/pccp](http://www.rsc.org/pccp)

## Introduction

Organic compounds are a major component of airborne particles.<sup>1–4</sup> A large fraction of the organic component under many circumstances is not from direct emissions, but rather is formed from low volatility products of the oxidation of volatile organic compounds (VOC) in air.<sup>5,6</sup> This introduces significant complexity in developing quantitative predictive models of atmospheric particulate matter, especially given the large number of potential precursors and oxidation processes. Models have typically under-predicted SOA mass compared to measurements; even with recent improvements,<sup>7–11</sup> accurately predicting specific characteristics such as O:C and volatility simultaneously remains a challenge.<sup>12</sup> However, given the key role of particles in affecting visibility,<sup>5,6,13</sup> health<sup>14–17</sup> and climate,<sup>18</sup> a detailed understanding of such processes is critical.

There are two important aspects to the formation of particles in the atmosphere: (1) how the initial seed particles are formed and (2) how they grow.<sup>19</sup> It is well established that sulfur compounds such as sulfuric and methanesulfonic acids form seed particles in the presence of ammonia, amines and water vapor.<sup>20–27</sup> Homogeneous nucleation of low volatility organic compounds is also a potential source of seed particles. As discussed in detail elsewhere,<sup>28–33</sup> for this to occur the compounds must have very low vapor pressures, recently dubbed ELVOC (extremely low VOC).<sup>30,34</sup> Biogenic precursors such as  $\alpha$ -pinene are expected to be particularly important because they have significant sources on a global basis and have structures and molecular masses such that oxidation leads to higher molecular weight, polar products that will have low volatility.

There is increasing evidence for homogeneous nucleation of large biogenic oxidation products. For example, the reaction of  $\text{O}_3$  with  $\alpha$ -pinene was shown using cluster chemical ionization mass spectrometry to generate gas phase oxidation products

Department of Chemistry, University of California, Irvine, CA 92697, USA.  
E-mail: [bjfinlay@uci.edu](mailto:bjfinlay@uci.edu); Fax: +1 949 824-7670; Tel: +1 949 824-2420

with molecular masses up to 621 amu.<sup>35</sup> Those with masses >430 amu were highly correlated with the formation of the smallest particles that were measured in that study (10 nm) while those with masses in the 140–380 amu range were correlated with larger particles (>20 nm).<sup>35</sup> Thermal desorption chemical ionization mass spectrometry (TD-CIMS) of particles formed in this reaction showed that 40 nm particles were comprised of more carbonyl-containing compounds and low molecular weight organic acids, while there was evidence of larger, lower vapor pressure acid products such as terpenylic and pinic acids in the 10 and 20 nm particles.<sup>36</sup> These data suggest that particles are initially formed by homogenous nucleation of ELVOC products, while subsequent growth occurs *via* uptake of products having smaller masses and relatively higher vapor pressures. In a similar system, correlations between gas phase ELVOC and SOA mass were observed both in the absence and presence of inorganic seed particles<sup>30</sup> and ELVOC adduct ions have been identified in chamber studies and ambient air.<sup>29</sup> High molecular weight oligomers have also been identified by high resolution mass spectrometric techniques.<sup>37–46</sup> Oligomerization is proposed to occur *via* acid catalyzed aldol and *gem*-diol reactions between SOA ‘monomers’,<sup>39,42,47,48</sup> generating esters, acetals and hemiacetals and/or the repeat addition of stabilized Criegee intermediates to peroxy radicals.<sup>41</sup>

The physical properties of SOA are still far from fully understood. While it was assumed for many years that SOA would be a relatively low viscosity liquid, a number of recent studies point to it being a semi-solid or even glassy material under certain conditions.<sup>32,49–68</sup> In this case diffusion of species will be much slower than in a liquid, which affects exchange with the gas phase and the growth mechanism for the particles. While diffusion coefficients ( $D$ ) for a given viscosity ( $\eta$ ) are often predicted through the Stokes–Einstein relationship that relates  $D$  inversely to  $\eta$ ,<sup>65,69</sup> this relationship has been shown to be inapplicable for water diffusing in highly viscous organic materials,<sup>70,71</sup> which likely includes SOA under some conditions. To date there has been only one direct measurement of diffusion in  $\alpha$ -pinene SOA, which is for pyrene incorporated into the SOA as it formed.<sup>66</sup>

We report here the results of studies, using a combination of experimental techniques, of the composition of particles from  $\alpha$ -pinene ozonolysis binned into two different size ranges (250–500 nm and >500 nm respectively) through the use of an impactor. Even with these larger particle sizes compared to the prior studies, there is clear evidence of enhancement of higher molecular mass components in the smaller size bin and more volatile components in the larger particles. The rates at which pinonaldehyde and acetic acid diffuse out of SOA deposited on a ZnSe surface are used to estimate the likely range of magnitudes of their diffusion coefficients. These are shown to be several orders of magnitude smaller than would be expected for liquid matrices<sup>65</sup> and hence are consistent with SOA from this reaction being a highly viscous material, in agreement with a growing body of evidence from this<sup>49,50</sup> and other laboratories.<sup>51–60,62–64,66</sup>

## Experimental

### SOA generation

SOA from the ozonolysis of  $\alpha$ -pinene under dry conditions was generated in our large volume, slow flow, aerosol flow tube<sup>72</sup> as has been described in detail previously.<sup>49,50,72</sup> Ozone ( $\sim 1$  ppm) was generated by flowing high purity oxygen (Oxygen Services, Ultra High Purity, 99.993%) through a housing containing a Pen-Ray<sup>®</sup> mercury lamp (UVP, LLC, model 11SC-2) and subsequently diluting to the desired concentration. The ozone concentration was monitored by Fourier transform infrared spectroscopy (FTIR, Mattson Instruments Inc., model 10000) and a photometric O<sub>3</sub> analyzer (Teledyne, model 400 E). The  $\alpha$ -pinene ((1R)-(+)- $\alpha$ -pinene; Sigma Aldrich, >99%) was added to the flow tube (after purification in an alumina column) downstream of the ozone inlet and was injected into the dilution airflow to the desired gas-phase concentration ( $\sim 1$  ppm) using an automated syringe pump (Pump Systems Inc., model NE-1000). The clean dry dilution air was from a purge gas air generator (Parker Balston, model 75-62), passed through carbon/alumina media (Perma Pure, LLC) and an inline 0.1  $\mu\text{m}$  filter (Headline Filters, DIF-N70). A scavenger for OH formed in the  $\alpha$ -pinene-ozone reaction<sup>5,73</sup> was not added in these experiments. The total flow rate in the flow tube was 34 L min<sup>-1</sup> corresponding to a total residence time of 33 minutes at the sampling port at the end of the flow tube. The particle size distributions were recorded using a scanning mobility particle sizer (SMPS, TSI, model 3080 classifier and 3776 condensation particle counter). The number mode diameter was 332 nm and the mass-weighted mode was 552 nm.

### ASAP-MS measurements

SOA was collected using a Sioutas impactor (SKC Inc.) with ZnSe substrates operated at 9 L min<sup>-1</sup>. Different stages were used to split the SOA into two size regimes of 250–500 nm and >500 nm. When collecting SOA between 250–500 nm the upper stage was greased (Dow Corning, high vacuum grease) to prevent larger particles bouncing down to the lower stage. The SOA was then physically transferred onto the tip of a glass melting point tube attached to an atmospheric solids analysis mass spectrometer probe (ASAP-MS)<sup>74,75</sup> (Waters). Prior to use, the melting point tube was cleaned by baking within the source at 450 °C for at least an hour. The mass spectrometer was a LCT Premier time-of-flight mass spectrometer (Waters) and was used in positive ion mode.

The source was operated at a constant temperature of 150 °C while temperature controlled nitrogen flowed over the tip (8.3 L min<sup>-1</sup>) to desorb the SOA components. The nitrogen temperature was manually ramped from 100 °C to 450 °C in a stepwise fashion in increments of 50 °C. The presence of a small container of liquid water in the source compartment resulted in the formation of H<sub>3</sub>O<sup>+</sup> ions by corona discharge and these undergo proton transfer reactions with the volatilized species to form [M + H]<sup>+</sup> ions. Mass spectra and total ion signals were acquired across 100–1000 Da as a function of temperature.

### ATR-FTIR measurements of the SOA

SOA was sampled using a custom designed impactor<sup>49</sup> with a ZnSe ATR (attenuated total reflectance) crystal substrate that had been cleaned prior to use by boiling in ethanol and dichloromethane before placing in an argon plasma for 30 min (Plasma Cleaner/Sterilizer PDC-32G, Harrick Scientific Products, Inc.). The polydisperse SOA was impacted at a flow rate of 30 L min<sup>-1</sup> for a total time of 5 minutes. The ATR impactor has a  $d_{50}$  cutoff diameter of  $240 \pm 12$  nm (ref. 49) at 30 L min<sup>-1</sup>, which captured most of the mass of the SOA.

IR spectra were recorded using a Nicolet™ 6700 FTIR spectrometer (Thermo Scientific). An ATR crystal was housed in a commercially available HATR (Horizontal ATR) accessory (PIKE Technologies, Madison WI). Background measurements of the clean crystal were recorded for subsequent analysis. Reference spectra of adsorbed and gas phase water were also taken by flowing humid air over the clean crystal (adsorbed) and into the sampling compartment of the spectrometer (gas-phase).

Once the polydisperse SOA was impacted onto the ATR crystal, the SOA covered crystal was transferred immediately to a custom designed flow cell<sup>76</sup> (volume 22 cm<sup>3</sup>) through which clean air was flowed. Infrared spectra of the SOA were recorded as single beam spectra and processed to give absorbance spectra in the form  $\log_{10}(S_0/S_1)$  where  $S_0$  represents a background relative to the spectrum of interest  $S_1$ . Spectra were recorded within ~5 min from the time of impaction and subsequent spectra were recorded every 15 minutes to monitor changes in the SOA under the flow (200 cm<sup>3</sup> min<sup>-1</sup>) of clean dry air (Oxygen Services, Ultra High Purity) for 20 hours.

### PTR-MS measurements of volatilized components

The outflow from the ATR flow cell was directed to a proton-transfer time-of-flight mass spectrometer (PTR-MS) (PTR-ToF-MS, Ionicon Analytik) to detect species evaporating from the SOA.

The PTR-MS acquisition was started prior to connecting the outflow of the ATR cell to the PTR-MS inlet *via* a 30 cm length of Teflon tubing. The moment of connection was taken as time  $t_0$ . Spectra were acquired at a rate of 3 scans per minute and were recorded for ~8 hours. Mass spectra were extracted using the PTR-MS TOF Viewer software (Ionicon Analytik version 1.4.0) by averaging a total of 10 individual scans starting close to  $t_0$ . Spectra after 8 hours in the clean air flow were used to determine the background. Peaks that increased significantly from this background were attributed to species evaporating from the SOA. The corresponding ion traces for the individual species were extracted after mass calibration.

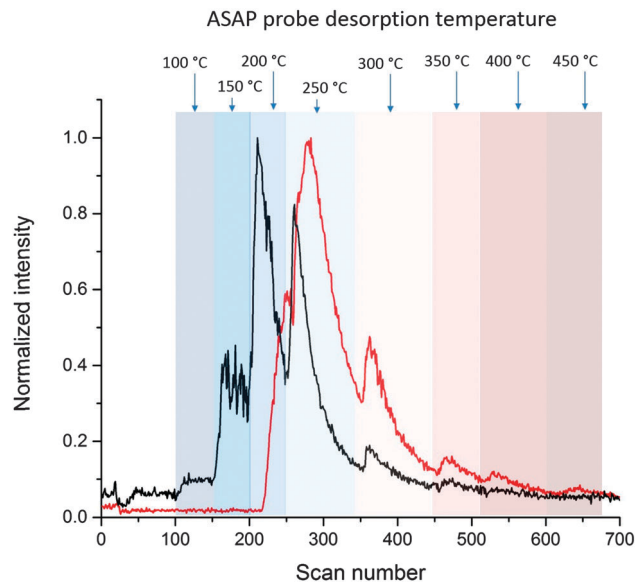
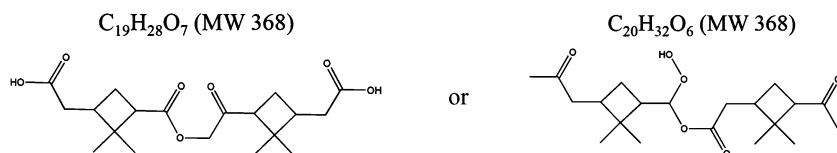


Fig. 1 Total ion signal (TIS) for ASAP-MS analysis of SOA from the ozonolysis of  $\alpha$ -pinene as a function of scan number and corresponding ASAP probe desorption temperature. The SOA was separated into fractions by particle size of 250–500 nm (red) and > 500 nm (black) by impaction prior to analysis. TIS have been peak normalized for comparison.

## Results and discussion

Fig. 1 shows typical ASAP-MS total ion signals for SOA in the smaller (250–500 nm; red curve) and larger (> 500 nm; black curve) size bins respectively as a function of scan number/desorption temperature. The signal for the larger SOA peaked at lower temperatures compared to that for the 250–500 nm SOA, indicating that some of its components are more volatile. The mass spectra were averaged (MassLynx™, Waters) to give a total integrated spectrum for the temperature range 100–450 °C for each sample. Six individual samples were analyzed for each size range (250 nm and > 500 nm). Fig. 2 shows a typical integrated ASAP mass spectrum for the 250–500 nm particles (Fig. 2a) and for the larger particles (Fig. 2b) (peaks highlighted in purple are observed in the background and hence were not included in subsequent quantitative analyses). It is clear that the smaller particles have a greater contribution to the total mass spectrum from higher molecular mass components, while peaks due to smaller products of this reaction are more evident in the larger particles. This is consistent with the higher volatility of the larger SOA seen in Fig. 1.

An obvious feature of the ASAP spectra is the strong peak at  $m/z = 351$ . This may be due to dehydrated  $[M + H - H_2O]^+$  fragments of previously proposed species with molecular weight of 368 amu:<sup>48,77</sup>



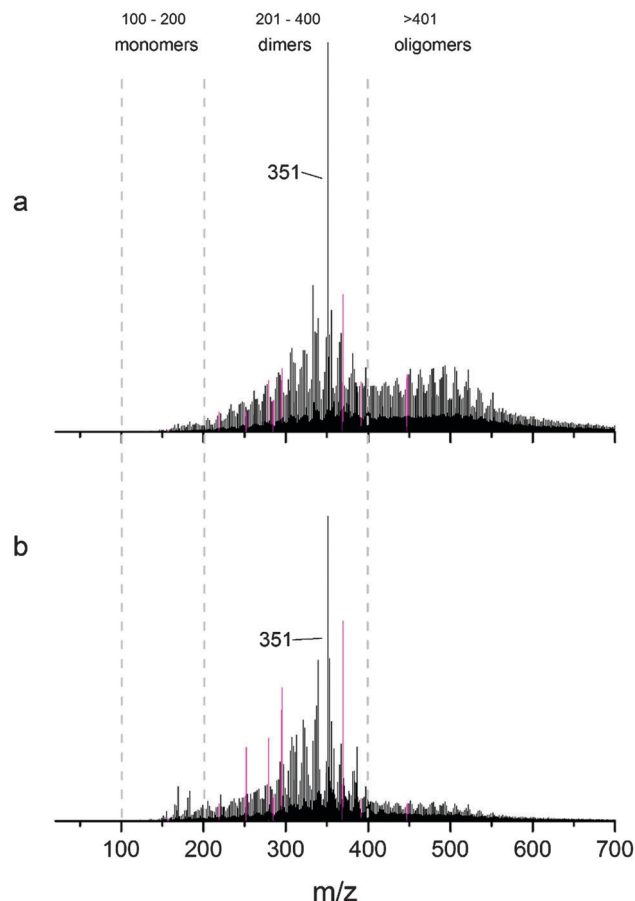


Fig. 2 Typical ASAP mass spectra of SOA from the ozonolysis of  $\alpha$ -pinene separated into size fractions of (a) 250–500 nm particles and (b) > 500 nm particles by a Sioutas impactor prior to analysis. The spectra have been normalized to the peak at an  $m/z$  of 351. The peaks highlighted in purple are observed in background spectra and are not included in quantitative analyses of the spectra. Dashed lines represent the boundaries for the quantitative analysis to assign to monomers, dimers, and oligomers. These boundaries are for illustrative purposes only.

The  $C_{19}H_{28}O_7$  diacid has been proposed to be formed from the reaction between pinic acid and 10-hydroxypinonic acid,<sup>48</sup> while the  $C_{20}H_{32}O_6$  hydroperoxide has been proposed to result from the reaction of a stabilized Criegee intermediate with pinonic acid<sup>77</sup> formed from the ozonolysis of  $\alpha$ -pinene. The relatively high intensity may indicate that such products are a major component of the SOA or alternatively, that the sensitivity to them in ASAP-MS is higher than for other components.

The integrated mass spectra were separated into mass ranges to represent SOA monomers (100–200 amu), dimers (201–400 amu) and oligomers (>401 amu) as illustrated in Fig. 2. These boundaries are not intended to be absolute assignments of monomeric, dimeric and oligomeric SOA components but rather to represent the mass ranges where such products are likely to be found. Fig. 3 shows the fraction of the total signal that falls into each mass range for the smaller particles (red boxes) compared to the > 500 nm particles (black boxes). As suggested qualitatively by the mass spectra (Fig. 2), the larger particles have a relatively greater contribution from

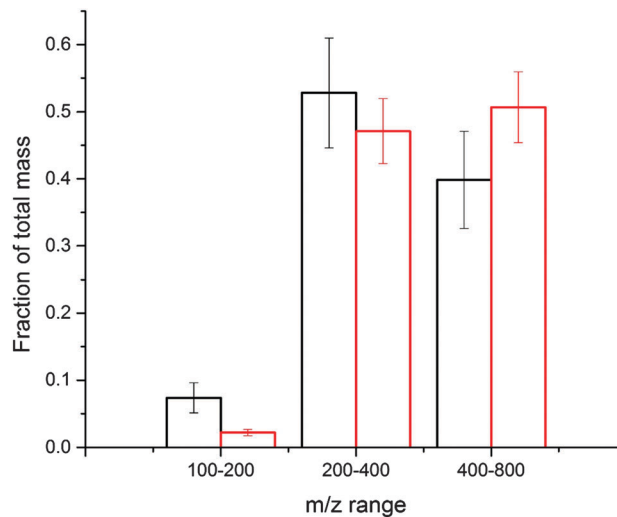


Fig. 3 Fraction of the total signal detected by ASAP-MS as a function of  $m/z$  range for SOA from the ozonolysis of  $\alpha$ -pinene. The SOA was separated into ranges by particle size of 250–500 nm (red) and > 500 nm (black) by impaction prior to analysis. Six individual spectra were analysed for each size bin and the fractions represent the average of the six measurements and associated  $1\sigma$  error. Contributions from contaminant peaks, highlighted in purple in Fig. 2, were subtracted from the integrals before calculating the relative fractions. The contribution from contaminants was of order 2–4% of the total signal detected.

low molecular mass components, while the smaller particles have more contribution from higher molecular masses.

Fig. 4a shows a typical ATR-FTIR spectrum of polydisperse SOA immediately following impaction. For comparison, ATR spectra of pinonic acid and pinonaldehyde identified in other studies<sup>78–93</sup> as common products of  $\alpha$ -pinene ozonolysis are also shown (Fig. 4b and c). As expected, the SOA spectrum exhibits significant similarities to those for these oxygenated products. Also shown in Fig. 4d is the difference spectrum for SOA after 20 hours under a flow of clean dry air. This spectrum is  $\log(S_1/S_{20})$  where  $S_1$  is the first single beam spectrum after introducing the flow of air and  $S_{20}$  is that after 20 hours, so that negative peaks represent functional groups lost from the SOA. The loss of  $C=O$  at  $1695\text{ cm}^{-1}$  is indicative of aldehydes/ketones that have evaporated from the SOA. The loss at  $\sim 3400\text{ cm}^{-1}$  could in part be due to a loss of carboxylic acids although the major contributor in this region is likely water which can be taken up during the brief handling in room air and then desorbed in the air flow. The change in this region was variable from experiment to experiment.

The difference spectrum also shows that there is a loss of species with peaks at  $1799$  and  $1768\text{ cm}^{-1}$  which were not obvious in the overall SOA spectrum (Fig. 4a) due to overlap with the strong  $1703\text{ cm}^{-1}$  peak (although a shoulder can be observed). There is also a loss of a peak at  $1072\text{ cm}^{-1}$ . Carbonyl groups with a more electronegative atom such as oxygen directly attached to the carbonyl carbon have the band due to the  $C=O$  stretching vibration shifted to higher frequencies than those for aldehydes and ketones that occurs around  $1700\text{ cm}^{-1}$ ; the same is true if the  $C=O$  is part of a strained ring.<sup>94</sup> In addition, if they are part of an ester or lactone, bands

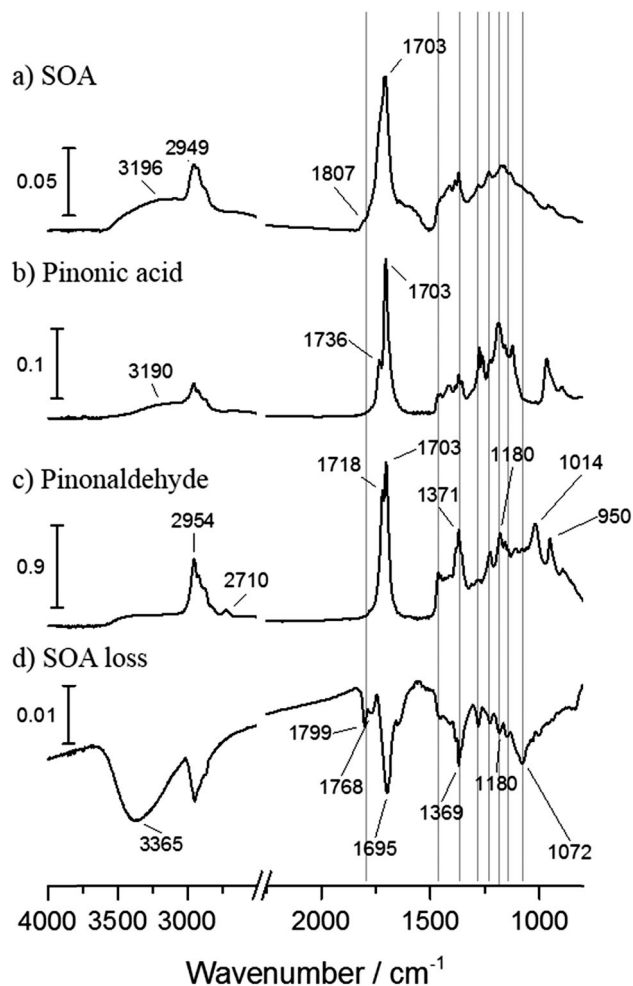
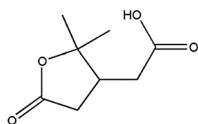


Fig. 4 (a) ATR-FTIR spectra of SOA from the ozonolysis of  $\alpha$ -pinene. Absorbance (y axis) is  $\log_{10}(S_0/S_1)$  where  $S_0$  is the single beam spectrum of a clean crystal and  $S_1$  the spectrum of the SOA covered crystal immediately following impaction. Contributions from gas-phase water have been subtracted; (b) and (c) are reference spectra of authentic samples of pinonic acid and pinonaldehyde. (d) Is the difference spectrum for SOA after 20 hours of clean air flow over the sample. This spectrum is  $\log_{10}(S_1/S_{20})$  where  $S_1$  is the spectrum of the SOA covered crystal immediately following impaction and  $S_{20}$  is that after 20 hours of clean air flow. Grey lines are to aid visual comparison between spectra.

due to the symmetric and asymmetric C(O)–O stretch appear in the 1050–1370  $\text{cm}^{-1}$  region.<sup>94</sup> Viable candidates for these bands in terms of  $\alpha$ -pinene ozonolysis products include the species responsible for the  $m/z = 351$  ASAP peak discussed earlier and/or terpenylic acid which has been previously identified as a product from the attack of OH on  $\alpha$ -pinene.<sup>95–97</sup> Anhydrides which have been reported in the ozonolysis of alkene self-assembled monolayers (SAMs)<sup>98</sup> are also a possibility.



Terpenylic acid (MW 172)

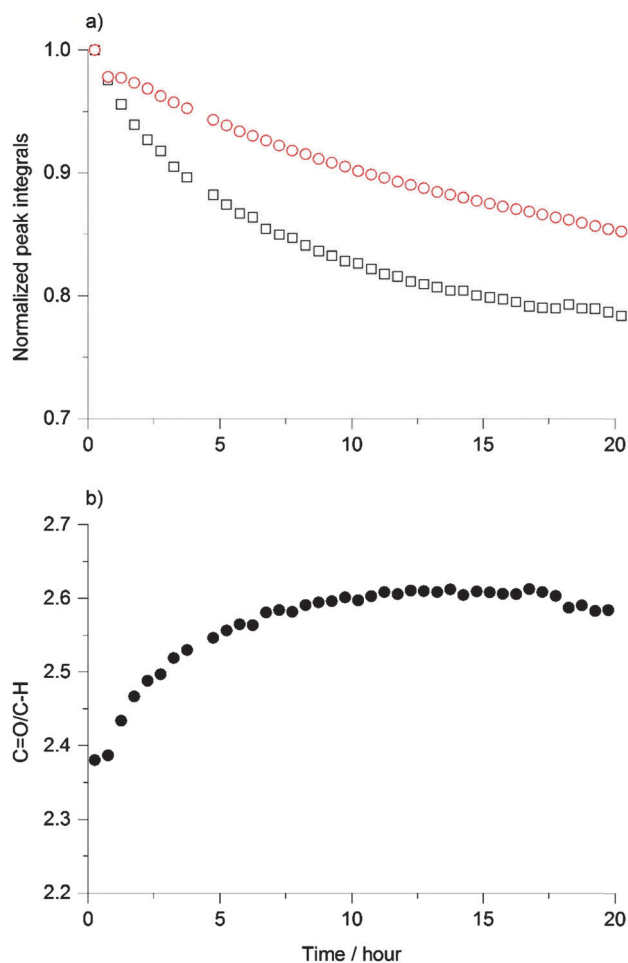


Fig. 5 (a) Normalized (at  $t = 0$ ) integrated C–H peak (open black squares) and C=O peak (open red circles) for SOA as a function of time under a flow of clean air. (b) Ratio of C=O to C–H of peak integrals as a function of time under a flow of clean dry air for SOA from the ozonolysis of  $\alpha$ -pinene. The C=O peak was the integrated area from 1658–1850  $\text{cm}^{-1}$ , but the peak at  $\sim 1700 \text{ cm}^{-1}$  dominates the signal. That for C–H was the integral from 2810–3050  $\text{cm}^{-1}$ .

Fig. 5a shows the loss of C=O and C–H groups under a flow of clean air for 20 hours which represents a decrease of  $\sim 20\%$  over this time. As seen in Fig. 5b, the ratio of the C=O to C–H peaks increased by  $\sim 10\%$  during evaporation of the SOA, as expected if more volatile, less oxygenated products were being removed by evaporation. Zelenyuk and co-workers<sup>62,66</sup> reported evaporative loss of  $\sim 70\%$  of  $\alpha$ -pinene ozonolysis SOA from individual particles up to several hundred nm in diameter over 24 hours. In the experiments reported here, the SOA forms a film on the crystal, the concentrations of the reactants were higher and no OH scavenger was added. The calculated depth of penetration of the infrared beam in the C–H stretch region at 2900  $\text{cm}^{-1}$  is 0.57  $\mu\text{m}$ , and at 1700  $\text{cm}^{-1}$  is 0.98  $\mu\text{m}$ .<sup>99</sup> As discussed below, the film is not evenly spread on the crystal but its thickness in some locations may be greater than the depth of penetration so that the observed evaporation (Fig. 5a) may be a lower limit. A contributing factor to the discrepancies in the evaporation may also be that in the earlier studies<sup>62,66</sup> there was

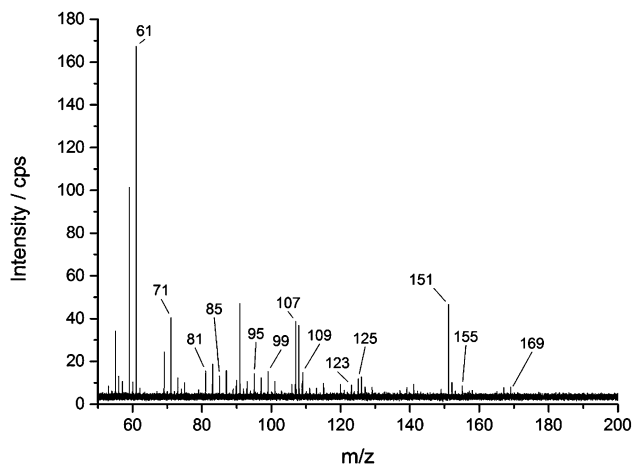


Fig. 6 PTR-MS spectrum of air flowing over SOA from  $\alpha$ -pinene ozonolysis. Spectrum is an average of 10 individual scans and is shown without background subtraction. Labelled peaks are those that were observable above the background. All other peaks in were present in background also and are therefore not assigned to species evaporating from SOA.

an initial rapid loss in the first few minutes during which more than  $\sim 20\%$  of the volume fraction was lost, followed by a smaller loss rate. The data in Fig. 5a were taken after the sample was removed from the impactor and installed in the flow cell, which took approximately 5 min. Thus a significant amount could have already evaporated by the time the first spectra were taken.

A search for gas phase products evaporating from the SOA on the ATR crystal was carried out using PTR-MS to sample from the exit of the flow cell. Fig. 6 shows the mass spectrum of this gas stream. Although PTR-MS is a softer ionization method than electron impact, it still results in significant fragmentation.<sup>100</sup> For example, pinonaldehyde (molecular mass 168) has a weak  $[M + H]^+$  peak at  $m/z = 169$  but a much stronger peak at  $m/z = 151$  corresponding to the addition of a proton and loss of water.<sup>87,101–107</sup> This makes definitive identification of gas phase products in complex mixtures difficult. However, the ratio of the peaks at  $m/z = 169/151$  that are characteristic of pinonaldehyde is within experimental error of that reported for this compound by Wisthaler *et al.*,<sup>101</sup> and the exact masses of the 151 and 169 peaks are within 25 ppm of those expected for this product. Carboxylic acids such as terpenylic acid readily lose water when they become protonated, which would give a peak at  $m/z = 155$  for the  $[M + H - H_2O]^+$  fragment. The PTR-MS peak at 155 was bimodal and could be resolved into two peaks which are tentatively assigned to: (1) terpenylic acid or norpinic acid dehydrated fragments ( $[M + H - H_2O]^+$ ,  $C_8H_{11}O_3$ , exact mass to 23 ppm) and (2) norpinonaldehyde ( $[M + H]^+$ ,  $C_9H_{15}O_2$ , exact mass to 28 ppm). The strong peak at  $m/z = 61$  corresponds to  $[M + H]^+$  for  $CH_3COOH$ <sup>100</sup> (acetic acid) which has previously been identified by PTR-MS as a gas phase product of the ozonolysis of  $\alpha$ -pinene<sup>87</sup> and for which there is also evidence in the particle phase.<sup>86</sup>

Fig. 7 shows the decays in the PTR-MS signals at  $m/z = 151$  and 61 respectively as clean air flowed over the SOA on the ATR

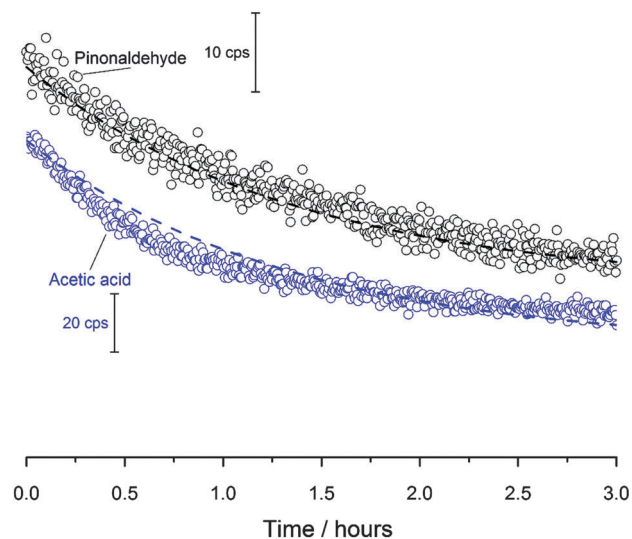


Fig. 7 PTR-MS time traces for  $m/z$  151 (black open circles) assumed to be pinonaldehyde, and  $m/z$  61 (blue open circles) assumed to be acetic acid, extracted from PTR-MS spectra of air flowing over SOA. The vertical bars give the scale for the signal intensity for the Y-axis in counts per second (cps). Dashed lines are fits to modelled diffusion assuming a  $D/l^2$  of  $5.0 \times 10^{-6} \text{ s}^{-1}$  for  $m/z$  151 and  $D/l^2$  of  $6.8 \times 10^{-6} \text{ s}^{-1}$  for  $m/z$  61 as described in the text.

crystal. In the simplest interpretation, these reflect primarily the time for the species to diffuse through the SOA matrix. While they also include the residence time in the ATR cell and travel time to the PTR-MS, these are of the order of tens of seconds and therefore negligible in comparison to the decay times seen in Fig. 7. As the  $m/z = 151$  and  $m/z = 61$  peaks are decaying on the timescale of hours, diffusion must be slow relative to that in liquids (where it would be effectively instantaneous on this experimental timescale),<sup>65</sup> suggestive of kinetic limitations in a highly viscous material. The decay of the  $m/z = 151$  and  $m/z = 61$  peaks, assumed to be due to pinonaldehyde and acetic acid respectively, were used to estimate the diffusion coefficients for these species in the SOA matrix.

If the generation of pinonaldehyde and acetic acid is limited only by diffusion in the SOA, then the process measured by the PTR-MS is similar to that used to determine diffusion coefficients,  $D$ , by outgassing from a sample.<sup>108</sup> For a thin film of thickness  $l$ , the time dependence of the amount of gas desorbing is an exponential of the form:<sup>108–110</sup>

$$\sum_{m=0}^{\infty} \frac{1}{(2m+1)^2} \exp\left[-\frac{D(2m+1)^2\pi^2 t}{l^2}\right]$$

The decay of the  $m/z = 151$  and 61 signals in Fig. 7 were fit to exponentials of this form, from which values of  $D/l^2$  can be derived. This approach gives  $D/l^2 = 5.0 \times 10^{-6} \text{ s}^{-1}$  for  $m/z = 151$  and  $6.8 \times 10^{-6} \text{ s}^{-1}$  for  $m/z = 61$ . The ratio of the diffusion coefficients for the species responsible for the 61 and 151 peaks in the PTR-MS data is therefore  $D_{61}/D_{151} = 1.4$ . We note that the fit to the  $m/z$  151 data is excellent over the entire course of the experiment out to 3 hours. The fit to  $m/z$  61 is not quite as good, which might reflect the fact that acetic acid is a sticky compound

which can adsorb/desorb to surfaces in the system. If the initial data to 2 hours for  $m/z$  61 is fit by the model, the value derived for  $D/l^2$  is  $9.0 \times 10^{-6} \text{ s}^{-1}$  and the ratio  $D_{61}/D_{151} = 1.8$ .

The Stokes–Einstein equation<sup>69</sup> which is often used to estimate diffusion coefficients predicts that the magnitude of the diffusion coefficient should vary inversely with the size of the diffusing molecule. The relative sizes of acetic acid and pinonaldehyde to which the peaks at 61 and 151 were assigned were calculated using the maximal estimate approach based on molar volumes.<sup>111</sup> The molar volume was calculated using the molecular weight of each species and the corresponding densities (a density of  $1.05 \text{ g cm}^{-3}$  was used for acetic acid and  $0.83 \text{ g cm}^{-3}$  for pinonaldehyde. In the absence of literature values for the density of pinonaldehyde, the density of non-aldehyde was used as an approximation.). The molecular diameter  $\sigma_v$  was calculated according to<sup>111</sup>

$$\sigma_v^3 = \frac{6V_M}{\pi N_A}$$

where  $V_M$  is the molar volume and  $N_A$  is Avagadro's number. The resulting estimated molecular diameters are 0.56 nm and 0.85 nm respectively for acetic acid and pinonaldehyde, suggesting the ratio of diffusion coefficients should be 1.5, in good agreement with the value of 1.4 derived from the data in Fig. 7.

The outgassing of pinonaldehyde and acetic acid could reflect not only diffusion in the SOA but also potentially their generation in the SOA through secondary chemistry. If the latter is comparable to or slower than diffusion, the rate of outgassing will be a combination of the kinetics of formation in the SOA and diffusion. The fact that the ratio of  $D/l^2$  for these two products is consistent with the ratio of their molecular sizes lends support to diffusion being the determining process in the outgassing. The Kelvin effect and capillary forces between particles have not been taken into account here because as discussed below (Fig. 8), the impacted sample forms a combination of large “spots” of many impacted particles and films of bounced particles where such effects will not be significant.

In order to derive absolute values of the diffusion coefficients, the film thickness  $l$  must be known. As shown recently in this laboratory,<sup>49</sup> and in Fig. 8, the SOA forms a complex pattern on the crystal due to some particles staying directly where the particles impact initially (centerline), with others bouncing towards the periphery of the crystal (cloud). If all the SOA were collected in the spot where they initially struck and stayed there, the maximum depth of SOA would be  $5 \mu\text{m}$ . It is clear from Fig. 8 that this is not the case as there is significant spreading across the whole crystal. If it were spread evenly over the crystal, it would form a film of thickness  $\sim 150 \text{ nm}$ .

As a result, there is no well-defined value of  $l$  that can be used to obtain the absolute value of the diffusion coefficients at this stage. Realistically,  $l$  could vary anywhere from 150 nm to a few microns. As an illustration, a film thickness of  $0.75 \mu\text{m}$  would lead to values of  $D$  of  $4 \times 10^{-14} \text{ cm}^2 \text{ s}^{-1}$  and  $3 \times 10^{-14} \text{ cm}^2 \text{ s}^{-1}$  for acetic acid and pinonaldehyde respectively. Taking into account the order of magnitude or so uncertainty in  $l$  (which will be the major source of error in any estimate of  $D$ ), this is still many orders of magnitude

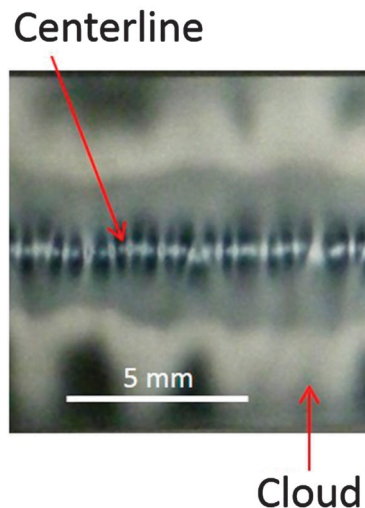


Fig. 8 Digital photograph of SOA impacted onto a Ge ATR crystal (scale bar = 5 mm) at  $30 \text{ L min}^{-1}$  for 5 minutes. Ge was used as ZnSe does not provide the contrast needed to photograph the SOA. The ATR crystal is  $8 \times 1 \text{ cm}$  (length by width) thus the photograph represents the full width of an SOA coated ATR crystal and a 1 cm portion of its length. The light color is impacted SOA and the dark colour is the Ge substrate. SOA particles impact initially at the centerline and may subsequently bounce forming the uneven coverage observed.

smaller than would be expected for a liquid matrix where diffusion coefficients of order  $10^{-5}$ – $10^{-10} \text{ cm}^2 \text{ s}^{-1}$  would be expected.<sup>65</sup> Abramson *et al.*,<sup>66</sup> made direct measurements of the diffusion of pyrene trapped in SOA particles during  $\alpha$ -pinene ozonolysis by measuring the pyrene remaining in particles after exposure to activated charcoal which takes up gas phase pyrene and other volatile organics. They obtained a diffusion coefficient for pyrene of  $2.5 \times 10^{-17} \text{ cm}^2 \text{ s}^{-1}$ . To our knowledge this<sup>66</sup> is the only direct measurement of a diffusion coefficient to date of an organic species within an SOA matrix. Their experiments were carried out with cyclohexane as an OH scavenger, which perceivably could result in SOA of a higher viscosity than in our experiments. Other factors that may contribute to the difference include that our studies involve flowing clean air over the SOA rather than depending on gas-phase diffusion from the gas–particle interface to a charcoal adsorbent at the bottom of the chamber. Diffusion coefficients may also be composition specific, depending not only on the size but also the nature of the diffusing species. The variable film thickness in our experiments limits our ability to estimate  $D$ , although no reasonable assumptions for this thickness would account for the magnitude of the differences observed. In any event, this highlights a real need for measurements of the diffusion coefficients of different organic species in SOA matrices with a variety of experimental techniques to improve our current understanding and ability to predict condensed phase kinetic limitations on diffusion of different organic species in SOA.

## Conclusions

SOA is a complex mixture of organic species which often exhibits behavior that challenges our assumptions of its composition and



physical properties. Developments in high-resolution soft ionization mass spectrometry techniques have, in recent years led to the detection of previously unknown components of and precursors to SOA such as oligomers<sup>37–46</sup> and ELVOC.<sup>29,30,35</sup> We have shown using a combination of infrared, and gas- and particle-phase mass spectrometry that smaller particles are less volatile and have larger high molecular weight fractions than larger particles. This is consistent with particle formation (in the absence of seed particles) by high molecular weight oligomers and ELVOC, and subsequent growth by condensation of smaller gas phase products. The evaporation rates of acetic acid and pinonaldehyde from SOA have been used to estimate the ratio of diffusion coefficients to the square of the average film thickness,  $D/l^2$  for acetic acid and pinonaldehyde, giving  $D/l^2 = 6.8 \times 10^{-6} \text{ s}^{-1}$  for acetic acid and  $5.0 \times 10^{-6} \text{ s}^{-1}$  for pinonaldehyde. Extracting absolute diffusion coefficients depends on assumptions made about the SOA film thickness. The relative magnitudes of these  $D/l^2$  are consistent with what would be expected based on the relative sizes of acetic acid and pinonaldehyde. Reasonable estimates of the film thickness of 150 nm to a few microns put the range of diffusion coefficients in the range consistent with SOA being a highly viscous material as indicated in previous studies.<sup>32,49–68</sup>

## Acknowledgements

The authors are grateful to the National Science Foundation (NSF), grant numbers 0909227 and 1207112 for support of this research, and the NSF Major Research Instrumentation (MRI) program (#0923323) for the PTR mass spectrometer. We also thank John Greaves of the University of California, Irvine Mass Spectrometry Facility for use of the ASAP-MS and technical advice.

## References

- J. L. Jimenez, M. R. Canagaratna, N. M. Donahue, A. S. H. Prevot, Q. Zhang, J. H. Kroll, P. F. DeCarlo, J. D. Allan, H. Coe, N. L. Ng, A. C. Aiken, K. S. Docherty, I. M. Ulbrich, A. P. Grieshop, A. L. Robinson, J. Duplissy, J. D. Smith, K. R. Wilson, V. A. Lanz, C. Hueglin, Y. L. Sun, J. Tian, A. Laaksonen, T. Raatikainen, J. Rautiainen, P. Vaattovaara, M. Ehn, M. Kulmala, J. M. Tomlinson, D. R. Collins, M. J. Cubison, J. Dunlea, J. A. Huffman, T. B. Onasch, M. R. Alfarra, P. I. Williams, K. Bower, Y. Kondo, J. Schneider, F. Drewnick, S. Borrmann, S. Weimer, K. Demerjian, D. Salcedo, L. Cottrell, R. Griffin, A. Takami, T. Miyoshi, S. Hatakeyama, A. Shimono, J. Y. Sun, Y. M. Zhang, K. Dzepina, J. R. Kimmel, D. Sueper, J. T. Jayne, S. C. Herndon, A. M. Trimborn, L. R. Williams, E. C. Wood, A. M. Middlebrook, C. E. Kolb, U. Baltensperger and D. R. Worsnop, *Science*, 2009, **326**, 1525–1529.
- J. Liggio, S. M. Li, A. Vlasenko, S. Sjostedt, R. Chang, N. Shantz, J. Abbatt, J. G. Slowik, J. W. Bottenheim, P. C. Brickell, C. Stroud and W. R. Leitch, *J. Geophys. Res.: Atmos.*, 2010, **115**, D21305.
- N. L. Ng, M. R. Canagaratna, Q. Zhang, J. L. Jimenez, J. Tian, I. M. Ulbrich, J. H. Kroll, K. S. Docherty, P. S. Chhabra, R. Bahreini, S. M. Murphy, J. H. Seinfeld, L. Hildebrandt, N. M. Donahue, P. F. DeCarlo, V. A. Lanz, A. S. H. Prevot, E. Dinar, Y. Rudich and D. R. Worsnop, *Atmos. Chem. Phys.*, 2010, **10**, 4625–4641.
- M. Hallquist, J. C. Wenger, U. Baltensperger, Y. Rudich, D. Simpson, M. Claeys, J. Dommen, N. M. Donahue, C. George, A. H. Goldstein, J. F. Hamilton, H. Herrmann, T. Hoffmann, Y. Iinuma, M. Jang, M. E. Jenkin, J. L. Jimenez, A. Kiendler-Scharr, W. Maenhaut, G. McFiggans, T. F. Mentel, A. Monod, A. S. H. Prévôt, J. H. Seinfeld, J. D. Surratt, R. Szmigielski and J. Wildt, *Atmos. Chem. Phys.*, 2009, **9**, 5155–5236.
- B. J. Finlayson-Pitts and J. N. Pitts, Jr., *Chemistry of the Upper and Lower Atmosphere – Theory, Experiments, and Applications*, Academic Press, San Diego, 2000.
- J. H. Seinfeld and S. N. Pandis, *Atmospheric Chemistry from Air Pollution to Climate Change*, Wiley, 2nd edn, 2006.
- A. G. Carlton, P. V. Bhave, S. L. Napelenok, E. D. Edney, G. Sarwar, R. W. Pinder, G. A. Pouliot and M. Houyoux, *Environ. Sci. Technol.*, 2010, **44**, 8553–8560.
- M. Shrivastava, J. Fast, R. Easter, W. I. Gustafson Jr, R. A. Zaveri, J. L. Jimenez, P. Saide and A. Hodzic, *Atmos. Chem. Phys.*, 2011, **11**, 6639–6662.
- K. M. Foley, S. J. Roselle, K. W. Appel, P. V. Bhave, J. E. Pleim, T. L. Otte, R. Mathur, G. Sarwar, J. O. Young, R. C. Gilliam, C. G. Nolte, J. T. Kelly, A. B. Gilliland and J. O. Bash, *Geosci. Model Dev.*, 2010, **3**, 205–226.
- A. P. Tsimpidi, V. A. Karydis, M. Zavala, W. Lei, L. Molina, I. M. Ulbrich, J. L. Jimenez and S. N. Pandis, *Atmos. Chem. Phys.*, 2010, **10**, 525–546.
- J. Fast, A. C. Aiken, J. Allan, L. Alexander, T. Campos, M. R. Canagaratna, E. Chapman, P. F. DeCarlo, B. de Foy, J. Gaffney, J. de Gouw, J. C. Doran, L. Emmons, A. Hodzic, S. C. Herndon, G. Huey, J. T. Jayne, J. L. Jimenez, L. Kleinman, W. Kuster, N. Marley, L. Russell, C. Ochoa, T. B. Onasch, M. Pekour, C. Song, I. M. Ulbrich, C. Warneke, D. Welsh-Bon, C. Wiedinmyer, D. R. Worsnop, X. Y. Yu and R. Zaveri, *Atmos. Chem. Phys.*, 2009, **9**, 6191–6215.
- K. Dzepina, C. D. Cappa, R. M. Volkamer, S. Madronich, P. F. DeCarlo, R. A. Zaveri and J. L. Jimenez, *Environ. Sci. Technol.*, 2011, **45**, 3496–3503.
- W. C. Hinds, *Aerosol Technology: Properties, Behavior and Measurement of Airborne Particles*, John Wiley & Sons Inc., New York, 1999.
- J. L. Mauderly and J. C. Chow, *Inhalation Toxicol.*, 2008, **20**, 257–288.
- C. A. Pope III and D. W. Dockery, *J. Air Waste Manage. Assoc.*, 2006, **56**, 709–742.
- M. R. Heal, P. Kumar and R. M. Harrison, *Chem. Soc. Rev.*, 2012, **41**, 6606–6630.
- U. Pöschl, *Angew. Chem., Int. Ed.*, 2005, **44**, 7520–7540.
- IPCC, Summary for Policymakers in: Climate Change 2013: The Physical Science Basis, Contribution of Working Group I to the Fifth Assessment Report of the Intergovernmental

- Panel on Climate Change, Cambridge University Press, Cambridge U.K., 2013.
- 19 R. Zhang, A. Khalizov, L. Wang, M. Hu and W. Xu, *Chem. Rev.*, 2011, **112**, 1957–2011.
  - 20 M. C. Facchini, S. Decesari, M. Rinaldi, C. Carbone, E. Finessi, M. Mircea, S. Fuzzi, F. Moretti, E. Tagliavini, D. Ceburnis and C. D. O'Dowd, *Environ. Sci. Technol.*, 2008, **42**, 9116–9121.
  - 21 V.-M. Kerminen, M. Aurela, R. E. Hillamo and A. Virkkula, *Tellus B*, 1997, **49**, 159–171.
  - 22 J. H. Zollner, W. A. Glasoe, B. Panta, K. K. Carlson, P. H. McMurry and D. R. Hanson, *Atmos. Chem. Phys.*, 2012, **12**, 4399–4411.
  - 23 J. N. Smith, K. C. Barsanti, H. R. Friedli, M. Ehn, M. Kulmala, D. R. Collins, J. H. Scheckman, B. J. Williams and P. H. McMurry, *Proc. Natl. Acad. Sci. U. S. A.*, 2010, **107**, 6634–6639.
  - 24 J. Kirkby, J. Curtius, J. Almeida, E. Dunne, J. Duplissy, S. Ehrhart, A. Franchin, S. Gagne, L. Ickes, A. Kurten, A. Kupc, A. Metzger, F. Riccobono, L. Rondo, S. Schobesberger, G. Tsagkogeorgas, D. Wimmer, A. Amorim, F. Bianchi, M. Breitenlechner, A. David, J. Dommen, A. Downard, M. Ehn, R. C. Flagan, S. Haider, A. Hansel, D. Hauser, W. Jud, H. Junninen, F. Kreissl, A. Kvashin, A. Laaksonen, K. Lehtipalo, J. Lima, E. R. Lovejoy, V. Makhmutov, S. Mathot, J. Mikkila, P. Minginette, S. Mogo, T. Nieminen, A. Onnela, P. Pereira, T. Petaja, R. Schnitzhofer, J. H. Seinfeld, M. Sipila, Y. Stozhkov, F. Stratmann, A. Tome, J. Vanhanen, Y. Viisanen, A. Vrtala, P. E. Wagner, H. Walther, E. Weingartner, H. Wex, P. M. Winkler, K. S. Carslaw, D. R. Worsnop, U. Baltensperger and M. Kulmala, *Nature*, 2011, **476**, 429–433.
  - 25 M. L. Dawson, M. E. Varner, V. Perraud, M. J. Ezell, R. B. Gerber and B. J. Finlayson-Pitts, *Proc. Natl. Acad. Sci. U. S. A.*, 2012, **109**, 18719–18724.
  - 26 T. Berndt, F. Stratmann, M. Sipilä, J. Vanhanen, T. Petäjä, J. Mikkilä, A. Grüner, G. Spindler, R. Lee Mauldin Iii, J. Curtius, M. Kulmala and J. Heintzenberg, *Atmos. Chem. Phys.*, 2010, **10**, 7101–7116.
  - 27 S. Angelino, D. T. Suess and K. A. Prather, *Environ. Sci. Technol.*, 2001, **35**, 3130–3138.
  - 28 A. H. Goldstein and I. E. Galbally, *Environ. Sci. Technol.*, 2007, 1283626.
  - 29 M. Ehn, E. Kleist, H. Junninen, T. Petäjä, G. Lönn, S. Schobesberger, M. Dal Maso, A. Trimborn, M. Kulmala, D. R. Worsnop, A. Wahner, J. Wildt and T. F. Mentel, *Atmos. Chem. Phys.*, 2012, **12**, 5113–5127.
  - 30 M. Ehn, J. A. Thornton, E. Kleist, M. Sipilä, H. Junninen, I. Pullinen, M. Springer, F. Rubach, R. Tillmann, B. Lee, F. Lopez-Hilfiker, S. Andres, I.-H. Acir, M. Rissanen, T. Jokinen, S. Schobesberger, J. Kangasluoma, J. Kontkanen, T. Nieminen, T. Kurtén, L. B. Nielsen, S. Jørgensen, H. G. Kjaergaard, M. Canagaratna, M. D. Maso, T. Berndt, T. Petäjä, A. Wahner, V.-M. Kerminen, M. Kulmala, D. R. Worsnop, J. Wildt and T. F. Mentel, *Nature*, 2014, **506**, 476–479.
  - 31 S. K. Friedlander, *Smoke and Dust Haze*, Oxford University Press, New York, 2nd edn, 2000.
  - 32 I. Riipinen, J. R. Pierce, T. Yli-Juuti, T. Nieminen, S. Häkkinen, M. Ehn, H. Junninen, K. Lehtipalo, T. Petäjä, J. Slowik, R. Chang, N. C. Shantz, J. Abbatt, W. R. Leitch, V. M. Kerminen, D. R. Worsnop, S. N. Pandis, N. M. Donahue and M. Kulmala, *Atmos. Chem. Phys.*, 2011, **11**, 3865–3878.
  - 33 M. Shrivastava, A. Zelenyuk, D. Imre, R. Easter, J. Beranek, R. A. Zaveri and J. Fast, *J. Geophys. Res.: Atmos.*, 2013, **118**, 3328–3342.
  - 34 N. M. Donahue, J. H. Kroll, S. N. Pandis and A. L. Robinson, *Atmos. Chem. Phys.*, 2012, **12**, 615–634.
  - 35 J. Zhao, J. Ortega, M. Chen, P. H. McMurry and J. N. Smith, *Atmos. Chem. Phys.*, 2013, **13**, 7631–7644.
  - 36 P. M. Winkler, J. Ortega, T. Karl, L. Cappellin, H. R. Friedli, K. Barsanti, P. H. McMurry and J. N. Smith, *Geophys. Res. Lett.*, 2012, **39**, L20815.
  - 37 M. Kalberer, D. Paulsen, M. Sax, M. Steinbacher, J. Dommen, A. S. H. Prevot, R. Fisseha, E. Weingartner, V. Frankevich, R. Zenobi and U. Baltensperger, *Science*, 2004, **303**, 1659–1662.
  - 38 M. P. Tolocka, M. Jang, J. M. Ginter, F. J. Cox, R. M. Kamens and M. V. Johnston, *Environ. Sci. Technol.*, 2004, **38**, 1428–1434.
  - 39 S. Gao, N. L. Ng, M. Keywood, V. Varutbangkul, R. Bahreini, A. Nenes, J. He, K. Y. Yoo, J. L. Beauchamp, R. P. Hodyss, R. C. Flagan and J. H. Seinfeld, *Environ. Sci. Technol.*, 2004, **38**, 6582–6589.
  - 40 D. S. Gross, M. E. Gälli, M. Kalberer, A. S. H. Prevot, J. Dommen, M. R. Alfarra, J. Duplissy, K. Gaeggeler, A. Gascho, A. Metzger and U. Baltensperger, *Anal. Chem.*, 2006, **78**, 2130–2137.
  - 41 A. Sadezky, R. Winterhalter, B. Kanawati, A. Rompp, B. Spengler, A. Mellouki, G. LeBras, P. Chaimbault and G. K. Moortgat, *Atmos. Chem. Phys.*, 2008, **8**, 2667–2669.
  - 42 W. A. Hall and M. V. Johnston, *J. Am. Soc. Mass Spectrom.*, 2012, **23**, 1097–1108.
  - 43 W. A. Hall and M. V. Johnston, *Aerosol Sci. Technol.*, 2011, **45**, 37–45.
  - 44 J. F. Hamilton, A. C. Lewis, T. J. Carey and J. C. Wenger, *Anal. Chem.*, 2008, **80**, 474–480.
  - 45 L. Müller, M. C. Reinnig, J. Warnke and T. Hoffmann, *Atmos. Chem. Phys.*, 2008, **8**, 1423–1433.
  - 46 K. J. Heaton, M. A. Dreyfus, S. Wang and M. V. Johnston, *Environ. Sci. Technol.*, 2007, **41**, 6129–6136.
  - 47 M. Jang, N. M. Czoschke, S. Lee and R. M. Kamens, *Science*, 2002, **298**, 814–817.
  - 48 F. Yasmeen, R. Vermeylen, N. Maurin, E. Perraudin, J.-F. Doussin and M. Claeys, *Environ. Chem.*, 2012, **9**, 236–246.
  - 49 C. Kidd, V. Perraud, L. M. Wingen and B. J. Finlayson-Pitts, *Proc. Natl. Acad. Sci. U. S. A.*, 2014, 7552–7557, DOI: 10.1073/pnas.1322558111.
  - 50 V. Perraud, E. A. Bruns, M. J. Ezell, S. N. Johnson, Y. Yu, M. L. Alexander, A. Zelenyuk, D. Imre, W. L. Chang,

- D. Dabdub, J. F. Pankow and B. J. Finlayson-Pitts, *Proc. Natl. Acad. Sci. U. S. A.*, 2012, **109**, 2836–2841.
- 51 T. D. Vaden, C. Song, R. A. Zaveri, D. Imre and A. Zelenyuk, *Proc. Natl. Acad. Sci. U. S. A.*, 2010, 6658–6663, DOI: 10.1073/pnas.0911206107.
- 52 C. D. Cappa and K. R. Wilson, *Atmos. Chem. Phys.*, 2011, **11**, 1895–1911.
- 53 M. Kuwata and S. T. Martin, *Proc. Natl. Acad. Sci. U. S. A.*, 2012, 17354–17359, DOI: 10.1073/pnas.1209071109.
- 54 L. Renbaum-Wolff, J. W. Grayson, A. P. Bateman, M. Kuwata, M. Sellier, B. J. Murray, J. E. Shilling, S. T. Martin and A. K. Bertram, *Proc. Natl. Acad. Sci. U. S. A.*, 2013, 8014–8019, DOI: 10.1073/pnas.1219548110.
- 55 E. Saukko, H. Kuuluvainen and A. Virtanen, *Atmos. Meas. Tech.*, 2012, **5**, 259–265.
- 56 A. Virtanen, J. Kannosto, H. Kuuluvainen, A. Arffman, J. Joutsensaari, E. Saukko, L. Hao, P. Yli-Pirila, P. Tiitta, J. K. Holopainen, J. Keskinen, D. R. Worsnop, J. N. Smith and A. Laaksonen, *Atmos. Chem. Phys.*, 2011, **11**, 8759–8766.
- 57 R. E. O'Brien, A. Neu, S. A. Epstein, A. C. MacMillan, B. Wang, S. T. Kelly, S. A. Nizkorodov, A. Laskin, R. C. Moffet and M. K. Gilles, *Geophys. Res. Lett.*, 2014, **41**, 4347–4353.
- 58 M. Shiraiwa, L. D. Yee, K. A. Schilling, C. L. Loza, J. S. Craven, A. Zuend, P. J. Ziemann and J. H. Seinfeld, *Proc. Natl. Acad. Sci. U. S. A.*, 2013, **110**, 11746–11750.
- 59 M. Shiraiwa and J. H. Seinfeld, *Geophys. Res. Lett.*, 2012, **39**, L24801.
- 60 C. D. Cappa and J. L. Jimenez, *Atmos. Chem. Phys.*, 2010, **10**, 5409–5424.
- 61 L. I. Kleinman, S. R. Springston, J. Wang, P. H. Daum, Y. N. Lee, L. J. Nunnermacker, G. I. Senum, J. Weinstein-Lloyd, M. L. Alexander, J. Hubbe, J. Ortega, R. A. Zaveri, M. R. Canagaratna and J. Jayne, *Atmos. Chem. Phys.*, 2009, **9**, 4261–4278.
- 62 T. D. Vaden, D. Imre, J. Beranek, M. Shrivastava and A. Zelenyuk, *Proc. Natl. Acad. Sci. U. S. A.*, 2011, **108**, 2190–2195.
- 63 E. Saukko, A. T. Lambe, P. Massoli, T. Koop, J. P. Wright, D. R. Croasdale, D. A. Pedernera, T. B. Onasch, A. Laaksonen, P. Davidovits, D. R. Worsnop and A. Virtanen, *Atmos. Chem. Phys.*, 2012, **12**, 7517–7529.
- 64 A. Virtanen, J. Joutsensaari, T. Koop, J. Kannosto, P. Yli-Pirilä, J. Leskinen, J. M. Mäkelä, J. K. Holopainen, U. Pöschl, M. Kulmala, D. R. Worsnop and A. Laaksonen, *Nature*, 2010, **467**, 824–827.
- 65 M. Shiraiwa, M. Ammann, T. Koop and U. Poschl, *Proc. Natl. Acad. Sci. U. S. A.*, 2011, **108**, 11003–11008.
- 66 E. Abramson, D. Imre, J. Beranek, J. Wilson and A. Zelenyuk, *Phys. Chem. Chem. Phys.*, 2013, **15**, 2983–2991.
- 67 T. Koop, J. Bookhold, M. Shiraiwa and U. Poschl, *Phys. Chem. Chem. Phys.*, 2011, **13**, 19238–19255.
- 68 B. Zobrist, C. Marcolli, D. A. Pedernera and T. Koop, *Atmos. Chem. Phys.*, 2008, **8**, 5221–5244.
- 69 K. J. Laidler and J. H. Meiser, *Physical Chemistry*, Longman, 1982.
- 70 R. M. Power, S. H. Simpson, J. P. Reid and A. J. Hudson, *Chem. Sci.*, 2013, **4**, 2597–2604.
- 71 H. C. Price, B. J. Murray, J. Mattsson, D. O'Sullivan, T. W. Wilson, K. J. Baustian and L. G. Benning, *Atmos. Chem. Phys.*, 2014, **14**, 3817–3830.
- 72 M. J. Ezell, S. N. Johnson, Y. Yu, V. Perraud, E. A. Bruns, M. L. Alexander, A. Zelenyuk, D. Dabdub and B. J. Finlayson-Pitts, *Aerosol Sci. Technol.*, 2010, **44**, 329–338.
- 73 R. Atkinson, S. M. Aschmann, J. Arey and B. Shorees, *J. Geophys. Res.: Atmos.*, 1992, **97**, 6065–6073.
- 74 E. A. Bruns, V. Perraud, J. Greaves and B. J. Finlayson-Pitts, *Anal. Chem.*, 2010, **82**, 5922–5927.
- 75 E. A. Bruns, J. Greaves and B. J. Finlayson-Pitts, *J. Phys. Chem. A*, 2012, **116**, 5900–5909.
- 76 S. G. Moussa and B. J. Finlayson-Pitts, *Phys. Chem. Chem. Phys.*, 2010, **12**, 9419–9428.
- 77 S. Lee and R. M. Kamens, *Atmos. Environ.*, 2005, **39**, 6822–6832.
- 78 T. S. Christoffersen, J. Hjorth, O. Horie, N. R. Jensen, D. Kotzias, L. L. Molander, P. Neeb, L. Ruppert, R. Winterhalter, A. Virkkula, K. Wirtz and B. R. Larsen, *Atmos. Environ.*, 1998, **32**, 1657–1661.
- 79 M. Glasius, M. Duane and B. R. Larsen, *J. Chromatogr. A*, 1999, **833**, 121–135.
- 80 M. Glasius, M. Lahaniati, A. Calogirou, D. Di Bella, N. R. Jensen, J. Hjorth, D. Kotzias and B. R. Larsen, *Environ. Sci. Technol.*, 2000, **34**, 1001–1010.
- 81 S. Hatakeyama, K. Izumi, T. Fukuyama and H. Akimoto, *J. Geophys. Res.: Atmos.*, 1989, **94**, 13013–13024.
- 82 T. Hoffmann, J. Odum, F. Bowman, D. Collins, D. Klockow, R. Flagan and J. Seinfeld, *J. Atmos. Chem.*, 1997, **26**, 189–222.
- 83 T. Hoffmann, R. Bandur, U. Marggraf and M. Linscheid, *J. Geophys. Res.: Atmos.*, 1998, **103**, 25569–25578.
- 84 J. Yu, R. C. Flagan and J. H. Seinfeld, *Environ. Sci. Technol.*, 1998, **32**, 2357–2370.
- 85 J. Yu, D. Cocker, III, R. Griffin, R. Flagan and J. Seinfeld, *J. Atmos. Chem.*, 1999, **34**, 207–258.
- 86 S. Koch, R. Winterhalter, E. Uherek, A. Koloff, P. Neeb and G. K. Moortgat, *Atmos. Environ.*, 2000, **34**, 4031–4042.
- 87 A. Lee, A. H. Goldstein, J. H. Kroll, N. L. Ng, V. Varutbangkul, R. C. Flagan and J. H. Seinfeld, *J. Geophys. Res.: Atmos.*, 2006, **111**, D17305.
- 88 R. Winterhalter, R. Van Dingenen, B. R. Larsen, N. R. Jensen and J. Hjorth, *Atmos. Chem. Phys. Discuss.*, 2003, **3**, 1–39.
- 89 M. Jang and R. M. Kamens, *Atmos. Environ.*, 1999, **33**, 459–474.
- 90 J. Warnke, R. Bandur and T. Hoffmann, *Anal. Bioanal. Chem.*, 2006, **385**, 34–45.
- 91 Y. Iinuma, O. Böge, T. Gnauk and H. Herrmann, *Atmos. Environ.*, 2004, **38**, 761–773.
- 92 Y. Iinuma, O. Boge, Y. Miao, B. Sierau, T. Gnauk and H. Herrmann, *Faraday Discuss.*, 2005, **130**, 279–294.
- 93 M. Jaoui, T. E. Kleindienst, M. Lewandowski, J. H. Offenberg and E. O. Edney, *Environ. Sci. Technol.*, 2005, **39**, 5661–5673.
- 94 G. Socrates, *Infrared and Raman Characteristic Group Frequencies: Tables and Charts*, John Wiley & Sons, West Sussex, 2007.

- 95 F. Yasmeen, R. Vermeylen, R. Szmigielski, Y. Iinuma, O. Böge, H. Herrmann, W. Maenhaut and M. Claeys, *Atmos. Chem. Phys.*, 2010, **10**, 9383–9392.
- 96 M. Claeys, Y. Iinuma, R. Szmigielski, J. D. Surratt, F. Blockhuys, C. Van Alsenoy, O. Böge, B. Sierau, Y. Gómez-González, R. Vermeylen, P. Van der Veken, M. Shahgholi, A. W. H. Chan, H. Herrmann, J. H. Seinfeld and W. Maenhaut, *Environ. Sci. Technol.*, 2009, **43**, 6976–6982.
- 97 A. Kahnt, Y. Iinuma, F. Blockhuys, A. Mutzel, R. Vermeylen, T. E. Kleindienst, M. Jaoui, J. H. Offenberg, M. Lewandowski, O. Böge, H. Herrmann, W. Maenhaut and M. Claeys, *Environ. Sci. Technol.*, 2014, **48**, 4901–4908.
- 98 L. R. Fiegand, M. McCorn Saint Fleur and J. R. Morris, *Langmuir*, 2005, **21**, 2660–2661.
- 99 N. J. Harrick, *Internal Reflection Spectroscopy*, John Wiley & Sons, 1967.
- 100 J. de Gouw and C. Warneke, *Mass Spectrom. Rev.*, 2007, **26**, 223–257.
- 101 A. Wisthaler, N. R. Jensen, R. Winterhalter, W. Lindinger and J. Hjorth, *Atmos. Environ.*, 2001, **35**, 6181–6191.
- 102 B. Warscheid and T. Hoffmann, *Atmos. Environ.*, 2001, **35**, 2927–2940.
- 103 P. Barmet, J. Dommen, P. F. DeCarlo, T. Tritscher, A. P. Praplan, S. M. Platt, A. S. H. Prévôt, N. M. Donahue and U. Baltensperger, *Atmos. Meas. Tech.*, 2012, **5**, 647–656.
- 104 S. Kim, T. Karl, A. Guenther, G. Tyndall, J. Orlando, P. Harley, R. Rasmussen and E. Apel, *Atmos. Chem. Phys.*, 2010, **10**, 1759–1771.
- 105 K. P. Wyche, A. C. Ryan, C. N. Hewitt, M. R. Alfarra, G. McFiggans, T. Carr, P. S. Monks, K. L. Smallbone, G. Capes, J. F. Hamilton, T. A. M. Pugh and A. R. MacKenzie, *Atmos. Chem. Phys. Discuss.*, 2014, **14**, 14291–14349.
- 106 Y. Yu, M. J. Ezell, A. Zelenyuk, D. Imre, L. Alexander, J. Ortega, B. D'Anna, C. W. Harmon, S. N. Johnson and B. J. Finlayson-Pitts, *Atmos. Environ.*, 2008, **42**, 5044–5060.
- 107 M. Camredon, J. F. Hamilton, M. S. Alam, K. P. Wyche, T. Carr, I. R. White, P. S. Monks, A. R. Rickard and W. J. Bloss, *Atmos. Chem. Phys.*, 2010, **10**, 2893–2917.
- 108 J. E. Shelby, *Handbook of Gas Diffusion in Solids and Melts*, ASM International, Materials Park, OH, 1996.
- 109 R. M. Barrer, *Diffusion In and Through Solids*, Cambridge University Press, Cambridge, England, 1941.
- 110 J. Crank, *The Mathematics of Diffusion*, Oxford University Press, London, England, 1964.
- 111 Y. Marcus, *J. Phys. Org. Chem.*, 2003, **16**, 398–408.